

Cite this: DOI: 10.1039/c0xx00000x

www.rsc.org/xxxxxx

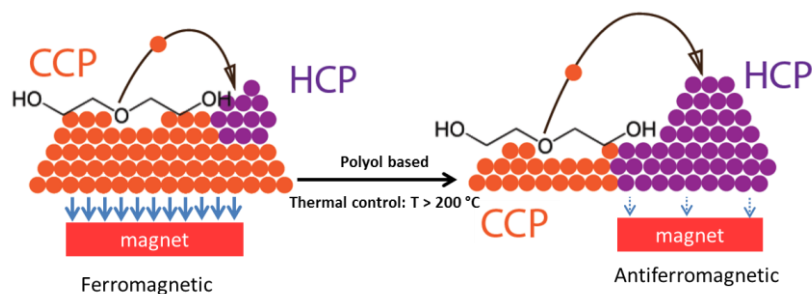
paper

Mechanism of polyol assisted *ccp* to *hcp* crystal phase conversion of nickel particles

Igor V. Sevonkaev, Ajeet Kumar, Angshuman Pal, and Dan V. Goia*

Received (in XXX, XXX) Xth XXXXXXXXXX 20XX, Accepted Xth XXXXXXXXXX 20XX

DOI: 10.1039/b000000x



The effect of different chain length glycols on the conversion of ferromagnetic *ccp* nickel nanoparticles to antiferromagnetic *hcp* structure was investigated. To be an effective crystal phase tuner, the glycol molecule must have both an ether fragment and a linear chain structure. The phase conversion was studied at reaction times up to 100 hours and temperatures between 200–275 °C. In selected conditions nickel particles of pure or mixed crystal structure could be generated.

Introduction

Ferromagnetic metals such as nickel, cobalt, and iron are widely used in a broad range of applications.^{1–9} Nickel, in particular, is the focus of extensive research due to its use in magnetic storage devices,^{10–12} biomedicine,^{13–16} multifunctional magnetic rotators,¹⁷ opto- and ferro-fluids,^{4, 18–21} electro-chemical organic catalysis,^{22–26} and batteries.^{27, 28}

Under normal conditions, nickel has a *ccp* structure (also known as a face-centered cubic or *fcc*) and exhibits ferromagnetic properties.²⁹ At temperatures in the 200–360 °C range, however, it can be converted to an antiferromagnetic *hcp* form.^{30–32} This has brought attention to the synthesis and characterization of *hcp* Ni particles because of their unique properties emanating from size, crystal structure, and mutual interactions.^{29, 30, 33–35}

To date, Ni particles with various sizes and shapes have been prepared by chemical reduction, sputtering,³⁶ thermal processes,^{32, 37, 38} reverse microemulsion technique,³⁹ and polyol mediated processes.^{30, 40–42} These methods typically yield Ni particles with either an *hcp* or a *ccp* crystal structure. In this paper we propose a versatile approach for controlling the conversion of *ccp* nickel to *hcp*, allowing the preparation of particles with a

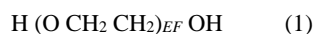
single crystal phase or a controlled degree of conversion from one phase to the other. The method at the core of this study was originally proposed by Kim et al.⁴³ While their work receives the merit for discovering the phenomenon, it did not elucidate the underlying mechanisms. The objective of this study was to fill this void and identify conditions for controlling the phase conversion by varying key process parameters. The approach described is simple, cost effective, creates only a mild environmental impact, and is capable of generating dispersed *hcp* particles at high metal concentrations.

Experimental

Materials and methods

The spherical nickel particles were received from Kawatetsu/Japan. They are essentially monocrystalline entities prepared using a chemical vapor deposition (CVD) process, having an average size of ~160 nm (Figure 1).

Water, glycerol (GL), 1,2-propane diol (PD), ethylene glycol (EG), di-ethylene glycol (Di-EG), tri-ethylene glycol (Tri-EG), and tetra-ethylene glycol (Tetra-EG) were the dispersion media selected for crystal phase conversion. The molecules of ethylene glycol, di-ethylene glycol, tri-ethylene glycol, and tetra-ethylene glycol can be schematically represented by the following general formula



where $EF = 1, 2, 3$ and 4 (Table 1). The fifth polyol is PD, the molecule that can be simplistically viewed as an ethylene glycol molecule in which one of the hydrogen atoms is replaced by a methyl group. The relevant information for the five polyols used

is given in Table 1.

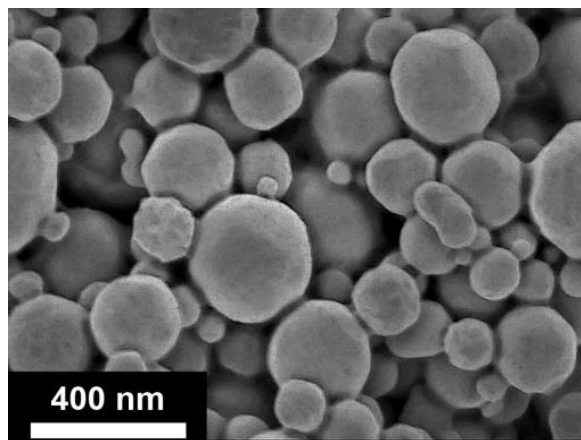
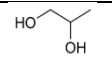
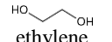
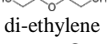
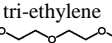
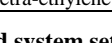


Figure 1. SEM image of original *ccp*-Ni particles

All polyols were obtained from Fluka and were used without further purification. The size and shape of nickel particles were determined by transmission (TEM JEM-2010) and field emission scanning (FESEM JEOL-7400) electron microscopy. Their crystal structure was assessed by X-Ray powder diffraction (XRD) using a Bruker-AXS D8 Focus X-ray diffractometer. The scanning step width was 0.01 degree, the step period 4 sec., while the source, sample, and detector slits were 2, 0.6, and 1 mm, respectively.

Table 1. Polyols used for the conversion of *ccp*-Ni into *hcp* at 275 °C for 18 h

Glycols	Boiling point, °C	No. of carbon	No. of ether fragments	<i>hcp</i> -phase conversion (%)
 propane diol	188	3	0	None
 ethylene glycol	197	2	0	7–10
 di-ethylene glycol	245	4	1	> 95
 tri-ethylene glycol	288	6	2	> 95
 tetra-ethylene glycol	329	8	3	> 95

15 Closed system setup

For each solvent, 0.5 g of Ni powder were introduced into a 100 ml high-pressure vessel containing 40 ml of solvent (Table 1). After an 18 hour incubation in the sealed reactor at 275 °C, the nickel particles were separated, washed, dried, and analyzed. This setup was necessary in order to maintain all solvents, for an extended time, at a temperature high enough (275 °C) to allow a measurable rate of phase conversion.

Open system setup

Ten grams of nickel powder were dispersed in 400 ml of Di-EG in a 500 ml round-bottom reactor. The reactor was placed in a heating mantle and the temperature was brought to either 200 °C or 225 °C. The nickel dispersions were maintained at the set temperature for up to 96 h under continuous stirring. Samples were extracted from the reactor at different times for XRD analysis.

Results and discussions

Metallic nickel can exist in either *ccp* (JCP-004-0850) or *hcp* (JCP-045-1027) crystal phases. The latter forms only within a specific temperature range (200–325 °C).³¹ Once *hcp*-Ni is formed, it is stable at temperatures below 325 °C but reverts back to *ccp* when the temperature is increased above 360 °C.³⁰⁻³²

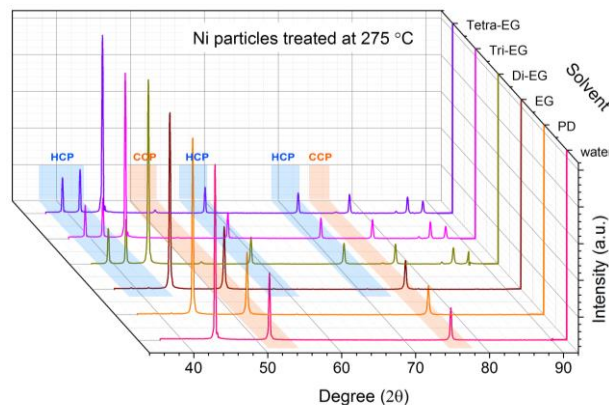


Figure 2. XRD patterns of Ni powders kept in different solvents at 275 °C for 18 h

Considering the metastable nature of the *hcp* phase, it is difficult to obtain by fast growth techniques (i.e. CVD, spray pyrolysis) Ni particles having a well-defined and controllable *ccp/hcp* ratio. However, it was previously shown that this can be achieved via slow phase transition taking place when Ni particles are kept for extended times in solvents that have sufficiently high boiling points. Polyols have been the preferred dispersion media for such studies.³¹ In their work, Tzitzios et al.³⁵ suggested that polyols with a higher molecular weight have elevated boiling points and are more effective in converting the Ni to an *hcp* structure. In this view, the temperature appears to be the only important process parameter. Our preliminary investigations however, revealed that the structure of the polyol molecule may be an even more critical factor in the conversion of Ni from the *ccp* to the *hcp* phase. The results of subsequent investigations presented here confirm this alternate view.

Table 2. Detailed XRD data for the Ni powders incubated at 275 °C for 18 hours in the solvents investigated

Phase	2 θ	hkl	Peak intensity, a.u.					
			Water	PD	EG	Di-EG	Tri-EG	Tetra-EG
<i>hcp</i>	39.28	010	n/a	n/a	30	716	917	1012
	41.63	002	n/a	n/a	40	916	1171	1279
<i>ccp</i>	51.82	200	2290	2515	2557	1005	n/a	100
<i>hcp</i>	58.56	012	n/a	n/a	n/a	513	664	750
	71.18	110	n/a	n/a	n/a	480	608	684
<i>ccp</i>	76.32	220	1219	1285	1290	532	n/a	70
<i>hcp</i>	78.10	103	n/a	n/a	10	494	621	660

To separate the effects of temperature and molecular structure of the glycols, we first heated for extended intervals the

dispersions of *ccp* Ni particles in solvents with a very broad range of boiling points. The treatment temperature (275 °C) was selected due to its median in the temperature range that favors the phase conversion.²⁷ In order to maintain the low boiling solvents at the set temperature, a closed system was used. When *ccp* Ni particles were kept for 18 h in the solvents listed in Table 1, the degree of conversion to *hcp* phase did not follow the expected trend based on their boiling points. As indicated by the XRD analysis (Figure 2 and Table 2), after incubation in either water or PG the structure of the Ni particles remained essentially unaffected.

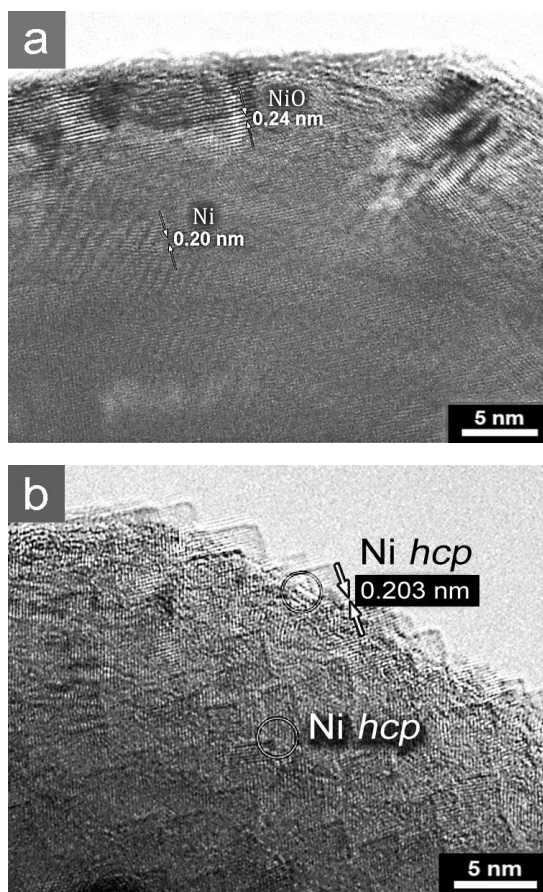


Figure 3 (a) TEM surface analysis of *ccp*-Ni particles reveals a thin (5–10 nm) NiO layer; (b) the superficial metal-oxide layer was converted into pyramidal *hcp*-Ni layer

The Rietveld refinement applied to the {2 0 0} crystallographic planes clearly indicated that the *hcp*-Ni crystal phase was not present. This means that the thermal re-arrangement of metal atoms did not occur for these two solvents.

For the sample kept in ethylene glycol (EG) only the structure and morphology of the outer particles' surface changed. The native thin layer of NiO (Figure 3a), estimated by high resolution TEM to have a thickness of 7 ± 3 nm and representing ~15% of the particle weight, was reduced by the solvent, forming a “pyramidal” *hcp*-Ni surface (Figure 3 b). Indeed, Rietveld refinement of the XRD data revealed that ~7–10% of *hcp*-Ni is present in the final powder. This suggests that the EG molecules reduced the nickel oxide to metallic nickel, which crystallized in an *hcp*-structure. The conversion did not, however, affect the core of the particles, which preserved the *ccp* structure.

In contrast, Ni powders kept in glycols with $EF = 2, 3$ and 4 underwent significant crystallographic and morphological changes. The XRD indicated that the entire body of the particles gradually re-crystallized in the *hcp* system. The characteristic peaks for the *ccp* system at 2θ (51.8° and 76.3°) have completely disappeared while those representative of the *hcp* phase (39.3°, 41.6°, 58.6°, and 71.2°) emerged (Figure 2 and Table 2). As can be seen from XRD in Figure 2, a small amount of *ccp*-Ni remained in the resulting powders. This may indicate that for a few very large Ni particles the phase conversion process did not reach their inner cores. The electron microscopy data revealed that the re-crystallized Ni particles had an entirely new morphology, changing in form from spherical to polygonal (Figure 4).

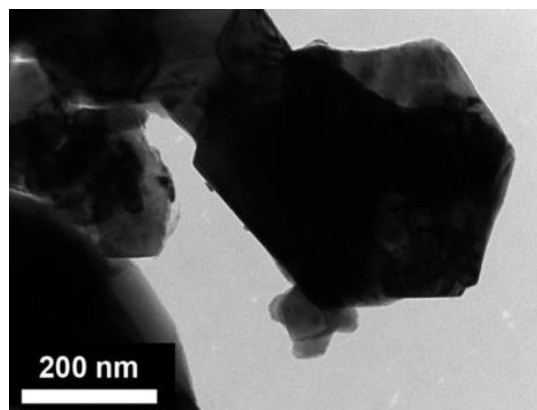


Figure 4. TEM image of a typical *hcp* Ni particles formed after 18 h at 275°C after incubation in glycols with $EF \geq 1$ (Eq. 1)

Both XRD data and TEM analysis (Figure 2–Figure 4), indicated that the *hcp* Ni particles obtained for all three polyols are highly crystalline. The calculated crystallite size determined by applying the Scherrer's equation to the (0 0 2) plane (Figure 5) is comparable with the particle size observed by electron microscopy (Figure 4). In the case of EG, however, the value is much smaller (~7 nm) as the conversion to *hcp* structure was confined to a thin surface layer (Figure 3b).

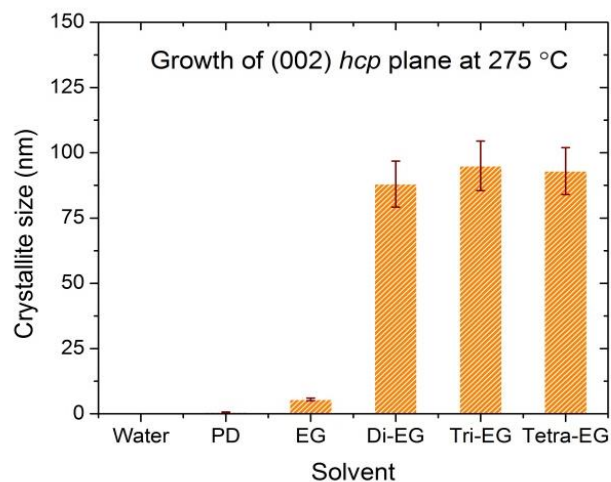


Figure 5. Calculated crystallite sizes corresponding to the (0 0 2) crystallographic plane of the formed *hcp*-Ni phase

Effect of time and temperature on Ni phase conversion

As indicated by the data above, any linear poly-glycol containing an ether fragment (-O-) may be used for Ni crystal phase conversion. Although solvents with a longer molecule chain appear to be more effective (i.e. shorter conversion times), Di-EG was selected as a dispersion medium for the open system for several reasons. First, since it has a high boiling point (245 °C), it provides an opportunity to work in an open vessel system. Second, Di-EG has the lowest viscosity of all glycols at ambient temperature⁴⁴ allowing easier separation of Ni particles. The evolution of the Ni particles crystal structure in Di-EG at 200 °C was monitored for 96 hours and evaluated by XRD (Figure 6). As shown by the diffractograms in Figure 6, there was no detectable structural change for the first 10 h. The characteristic peaks for the *hcp* phase start to emerge in the XRD patterns after ~18 h and continue to increase gradually in intensity for the next 78 h.

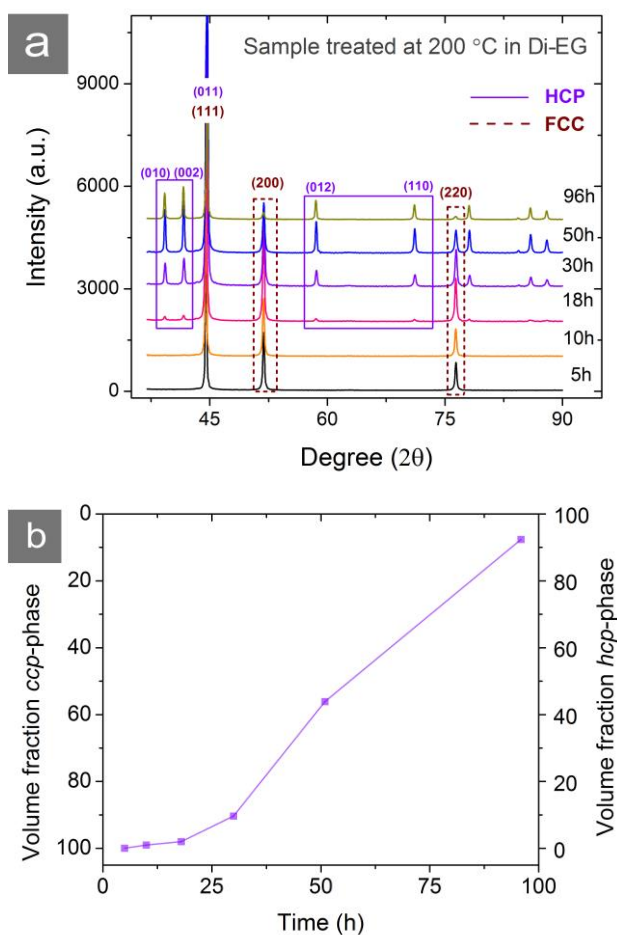


Figure 6. (a) Evolution of *ccp* to *hcp*-Ni particles crystal phase at 200 °C; and (b) *ccp* to *hcp* conversion rate

The ratio of the (2 0 0) peak of the *ccp* phase (i.e., near $2\theta = 51.83^\circ$) and the (0 0 2) reflection of the *hcp* phase was used to estimate the rate of *ccp*-to-*hcp* conversion (Figure 6 b). Based on this plot, conditions needed for a desired ratio of the two phases can be easily identified. When Ni particles were kept in Di-EG at 225 °C, it took only 24 h to convert a larger fraction of the Ni *ccp* into the *hcp* phase (Figure 7).

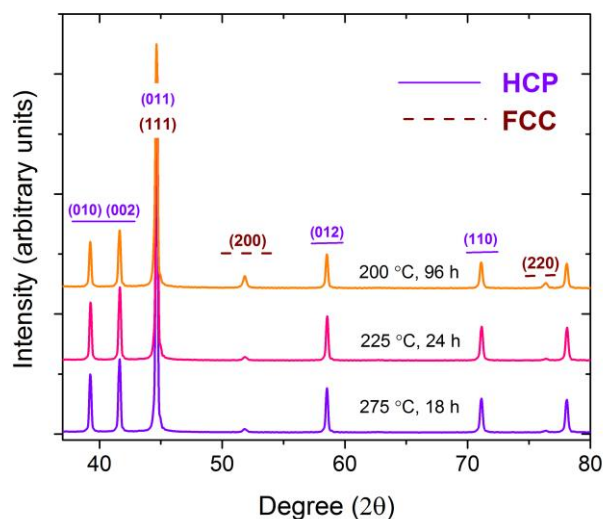


Figure 7. Effect of temperature on the conversion of *ccp*-Ni to *hcp* in Di-EG

Mechanism of nickel conversion from *ccp* to *hcp*

Based on the data presented, we propose the following mechanism for Ni crystal phase conversion in polyols. The essential element of the new view is: in order to be both a reducing agent and an efficient crystal phase tuner, the glycol molecule must contain an ether fragment. It is known that the hydroxyl groups of any polyol efficiently bind to the metal oxide surface⁴⁵ and reduce it to metallic nickel by lowering the surface activation energy of the redox reaction.³⁵ Indeed, a polyol without an ether group (propane diol) reduces the nickel oxide layer but the resulting metal atoms adopt the same *ccp* structure as the particle core, which acts as a template for their spatial arrangement. As a result, the XRD pattern contains only peaks characteristic for the *ccp* phase. On the other hand, glycols that possess at least one ether group, manage to not only reduce the NiO superficial layer, but also re-arrange the atoms of both, surface and particle core from a *ccp* to an *hcp* configuration. The likely mechanism of this phase transformation is through 'dislodging' and transport of Ni atoms from locations in the *ccp* crystal to new locations where the atoms adopt the *hcp* arrangement. This may occur by either a surface diffusion⁴⁶ or 'dissolution-precipitation' mechanism. The rearrangement of the atoms is presented schematically in Figure 8, which is inline with TEM data in Figure 3b.

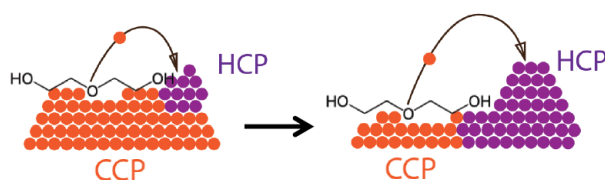


Figure 8. Schematic mechanism of the re-arrangement of Ni atoms from a *ccp* to an *hcp* configuration

In both cases it is evident that the -O- groups play an essential role in ensuring the transport and rearrangement of Ni atoms. It also appears that an increased number of -O- fragments in the molecule increases the efficiency of the Ni atom transport from

the *ccp* to the *hcp* locations. This is clearly confirmed by the trend in the intensity of the *hcp* reflections in Table 2.

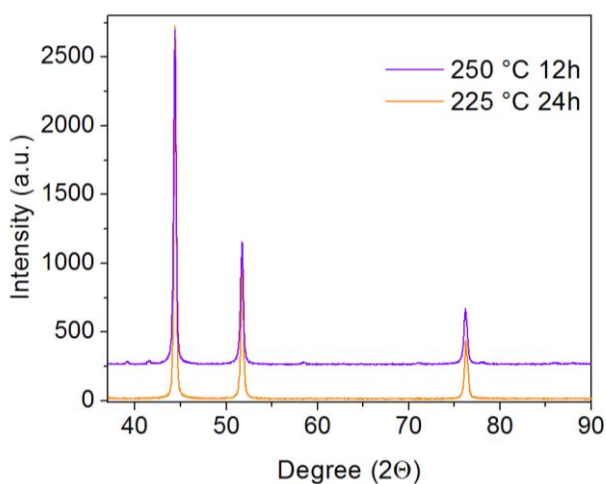


Figure 9. XRD pattern of Ni particles maintained in glycerol at 250 °C for 12 hours (top) and 225 °C for 24 hours (bottom)

Ethylene glycol presents an interesting case, where the conversion is restricted to the superficial layer of atoms resulting from the reduction of Ni²⁺ ions from NiO. Although, as PD, ethylene glycol molecules do not contain an ether fragment, they can react in the conditions of the experiment (high temperature and the presence of a metal surface with catalytic properties) to form dimers that do possess the –O– group capable of facilitating the rearrangement of superficial Ni atoms. The process is slow, however, since the concentration of the –O– containing dimers formed is much lower than the concentration of in the three polyols already containing this moiety in their molecule. In the case of PD, which has only one terminal carbon containing an OH group, the probability of collisions that lead to water elimination and the formation of –O– fragments is drastically reduced. In the absence of a significant number of –O– containing groups, the atoms resulting from the reduction of the NiO layer are deposited in the same *ccp* arrangement as the subsurface core template. A further confirmation of the essential role of the intra-molecular ether groups in the phase conversion was provided by experiments carried out in glycerol. This polyol has a very high boiling point (290 °C) and, according to the previous view that only a high temperature is needed, should be a very effective phase conversion promoter. Our investigations however, revealed that with incubation in the open system under the same conditions of temperature (225 °C) and time (24 h) as for Di-EG, conversion from *ccp* to *hcp* is negligible (Figure 9, orange plot). Even at a higher temperature (250 °C), the conversion of Ni atoms from the NiO layer to *hcp* structure (Figure 9, violet plot) can hardly be observed. This suggests that the etherification process at these temperatures is negligible. This behaviour can most likely be attributed to the following factors: the incubation was carried out at a much lower temperature than the boiling point of glycerol and an –OH group was present between the terminal hydroxyl groups.

Conclusions

This study presents a simple and convenient method for changing the structure of crystalline nickel particles from *ccp* to *hcp* in a controllable manner. The conversion of Ni lattice was investigated at high temperature in various polyols. In contrast with the findings of previous studies, we have shown that the structure of glycol molecules, and not the temperature at which the conversion is carried out, is the most critical factor in the recrystallization of Ni. For this purpose, polyols with different structure and boiling points were used as solvents for phase conversion. We have shown that, in order to be effective as a phase changer, the polyol molecule must be linear and contain at least one ether fragment. The –O– moiety is responsible for the mobility of Ni atoms in the *ccp* lattice and their transport and rearrangement into distinct crystalline entities having an *hcp* structure. Effectiveness of the phase conversion increases with the number of –O– fragments in the polyol molecule. Polyols not containing an ether fragment are largely ineffective as phase tuners. Exceptions are the linear polyols with two terminal hydroxyl groups, which during the high temperature process can dimerize and form in situ –O– groups. However, given the low concentration of these species, the conversion process is confined to the surface of the particles.

Acknowledgements

Authors are grateful for financial support from Umicore AG (Hanau/Germany). We also acknowledge the valuable discussions with Prof. Vladimir Privman (Clarkson University), Dr. Alexandr Trotsenko, and Brandon Bartling of GE Global Research (Niskayuna, NY).

Notes and references

- ^a *Center for Advanced Materials Processing, Department of Chemistry and Biomolecular Science, Clarkson University, Potsdam, NY 13699, USA. Tel: +1 315 268 4411, E-mail: goitadvn@clarkson.edu
1. S. Sun and C. B. Murray, *J. Appl. Phys.*, 1999, **85**, 4325-4330.
 2. V. F. Puentes, K. M. Krishnan and A. P. Alivisatos, *Science*, 2001, **291**, 2115-2117.
 3. O. Santini, A. R. de Moraes, D. H. Mosca, P. E. N. de Souza, A. J. A. de Oliveira, R. Marangoni and F. Wypych, *J. Colloid Interface Sci.*, 2005, **289**, 63-70.
 4. N. Pamme, *Lab Chip*, 2006, **6**, 24-38.
 5. S. P. Gubin, Y. I. Spichkin, G. Y. Yurkov and A. M. Tishin, *Russ. J. Inorg. Chem.*, 2002, **47**, S32-S67.
 6. N. V. Myung, D. Y. Park, B. Y. Yoo and P. T. A. Sumodjo, *J. Magn. Mater.*, 2003, **265**, 189-198.
 7. S. Rana, A. Gallo, R. S. Srivastava and R. D. K. Misra, *Acta Biomater.*, 2007, **3**, 233-242.
 8. S. Feihl, R. D. Costa, S. Pflock, C. Schmidt, J. Schönamsgruber, S. Backes, A. Hirsch and D. M. Guldi, *RSC Advances*, 2012, **2**, 11495-11503.
 9. M. Vaseem, N. Tripathy, G. Khang and Y.-B. Hahn, *RSC Advances*, 2013, **3**, 9698-9704.
 10. S. Zahi, *Materials & Design*, 2010, **31**, 1848-1853.
 11. C. Gong, L. Yu, Y. Duan, J. Tian, Z. Wu and Z. Zhang, *Eur. J. Inorg. Chem.*, 2008, 2884-2891.
 12. Q. Chen and D. H. Yao, *Asian J. Chem.*, 2013, **25**, 3366-3368.
 13. M. Bettge, J. Chatterjee and Y. Haik, *Biomagn. Res. Technol.*, 2004, **2**, 4.
 14. M. Ahamed, M. J. Akhtar, M. A. Siddiqui, J. Ahmad, J. Musarrat, A. A. Al-Khedhairi, M. S. AlSalhi and S. A. Alrokayan, *Toxicology*, 2011, **283**, 101-108.
 15. J. Klostergaard and C. E. Seeney, *Maturitas*, 2012, **73**, 33-44.

-
16. S. Rodriguez-Llamazares, J. Merchan, I. Olmedo, H. P. Marambio, J. P. Munoz, P. Jara, J. C. Sturm, B. Chornik, O. Pena, N. Yutronic and M. J. Kogan, *J. Nanosci. Nanotechnol.*, 2008, **8**, 3820-3827.
 17. A. Tokarev, A. Aprelev, M. N. Zakharov, G. Korneva, Y. Gogotsi and K. G. Kornev, *Rev. Sci. Instrum.*, 2012, **83**, 065110-065118.
 18. S. Z. Malynych, A. Tokarev, S. Hudson, G. Chumanov, J. Ballato and K. G. Kornev, *J. Magn. Magn. Mater.*, 2010, **322**, 1894-1897.
 19. A. Tokarev, B. Rubin, M. Bedford and K. G. Kornev, *AIP Conf. Proc.*, 2010, **1311**, 204-209.
 20. K. Griesar, Y. Galyametdinov, M. Athanassopoulou, I. Ovchinnikov and W. Haase, *Adv. Mater.*, 1994, **6**, 381-384.
 21. V. Bonanni, S. Bonetti, T. Pakizeh, Z. Pirzadeh, J. Chen, J. Nogués, P. Vavassori, R. Hillenbrand, J. Åkerman and A. Dmitriev, *Nano Lett.*, 2011, **11**, 5333-5338.
 22. A. Alejandre, F. Medina, P. Salagre, A. Fabregat and J. E. Sueiras, *Appl. Catal., B*, 1998, **18**, 307-315.
 23. T. Minowa and T. Ogi, *Catal. Today*, 1998, **45**, 411-416.
 24. R. N. Widyaningrum, T. L. Church, M. Zhao and A. T. Harris, *Int. J. Hydrogen Energy*, 2012, **37**, 9590-9601.
 25. J. Wang, G. Fan and F. Li, *RSC Advances*, 2012, **2**, 9976.
 26. G. Chen, Y. Zhao, D. Lv, T. Zhao, Y. Zhu and Y. Sun, *RSC Advances*, 2013, **3**, 5314-5317.
 27. C.-H. Dustmann, *J. Power Sources*, 2004, **127**, 85-92.
 28. C. D. Wessells, S. V. Peddada, R. A. Huggins and Y. Cui, *Nano Lett.*, 2011, **11**, 5421-5425.
 29. Y. T. Jeon, J. Y. Moon, G. H. Lee, J. Park and Y. Chang, *J. Phys. Chem. B*, 2006, **110**, 1187-1191.
 30. C. N. Chinnasamy, B. Jeyadevan, K. Shinoda, K. Tohji, A. Narayanasamy, K. Sato and S. Hisano, *J. Appl. Phys.*, 2005, **97**, 10J309.
 31. J. Gong, Y. Liu, L. Wang, J. Yang and Z. Zong, *Front. Chem. China*, 2008, **3**, 157-160.
 32. Y. Mi, D. Yuan, Y. Liu, J. Zhang and Y. Xiao, *Mater. Chem. Phys.*, 2005, **89**, 359-361.
 33. A. Kotoulas, M. Gjoka, K. Simeonidis, I. Tsiaoussis, M. Angelakeris, O. Kalogirou and C. Dendrinou-Samara, *J. Nanopart. Res.*, 2011, **13**, 1897-1908.
 34. K. S. Rao, T. Balaji, Y. Lingappa, M. R. P. Reddy and T. L. Prakash, *Phase Transitions*, 2012, **85**, 235-243.
 35. V. Tzitzios, G. Basina, M. Gjoka, V. Alexandrakis, V. Georgakilas, D. Niarchos, N. Boukos and D. Petridis, *Nanotechnology*, 2006, **17**, 3750-3755.
 36. J. Higuchi, M. Ohtake, Y. Sato, T. Nishiyama and M. Futamoto, *Jpn. J. Appl. Phys.*, 2011, **50**, 063001.
 37. M. Liu, J. Chang, J. Sun and L. Gao, *RSC Advances*, 2013, **3**, 8003.
 38. M. Shviro and D. Zitoun, *RSC Advances*, 2013, **3**, 1380-1387.
 39. A. Kumar, A. Saxena, A. De, R. Shankar and S. Mozumdar, *Adv. Nat. Sci.: Nanosci. Nanotechnol.*, 2013, **4**, 025009.
 40. F. Fievet, J. P. Lagier, B. Blin, B. Beaudoin and M. Figlarz, *Solid State Ionics*, 1989, **32-33, Part 1**, 198-205.
 41. T. Hinotsu, B. Jeyadevan, C. N. Chinnasamy, K. Shinoda and K. Tohji, *J. Appl. Phys.*, 2004, **95**, 7477-7479.
 42. US20120238443 A1, 2012.
 43. US7211126 B2, 2007.
 44. J. Jądzyn, G. Czechowski and T. Stefaniak, *J. Chem. Eng. Data.*, 2002, **47**, 978-979.
 45. S. Takeda, M. Fukawa, Y. Hayashi and K. Matsumoto, *Thin Solid Films*, 1999, **339**, 220-224.
 46. I. Sevonkaev, V. Privman and D. Goia, *J. Chem. Phys.*, 2013, **138**, 014703-014706.